Japanese Journal of Radiology (2018) 36:134–141
https://doi.org/10.1007/s11604-017-0705-0

ORIGINAL ARTICLE

MRI findings for primary fallopian tube cancer: correlation with pathological findings

Satomi Kitai[1] · Takako Kiyokawa[1] · Yumiko O. Tanaka[1] · Kaoru Onoue[1] · Hiroyuki Takahashi[1] · Motoaki Saitou[1] · Aikou Okamoto[1] · Kunihiko Fukuda[1]

Received: 13 June 2017 / Accepted: 7 November 2017 / Published online: 18 November 2017

Abstract

Purpose To clarify the MRI findings for primary fallopian tube cancer (PFTC).

Materials and methods MRI findings for 11 patients who were pathologically diagnosed with PFTC at our institute were retrospectively reviewed. MRI findings (shape, appearance, signal intensity, ADC value, enhancement patterns, and location of the primary tumor, the morphologic appearance of the ipsilateral ovary, and intrauterine fluid collection) were evaluated and compared with pathological findings including histological subtype and PFTC location.

Results On MRI, PFTCs with a tubal component ($n = 8$) exhibited a sausage-like shape in five cases and a nodular or irregular shape in three cases. PFTCs located at the fimbria ($n = 3$) presented a nodular shape. The PFTC was solid in nine cases (82%), and the solid portion showed high intensity on diffusion-weighted images in all cases. The mean ADC value was 0.86×10^{-3} mm^2/s. Rim enhancement of the tumor was seen in six of nine cases (67%), all with a tubal component.

Conclusion PFTCs with a tubal component are sausage-shaped and PFTCs located at the fimbria have a nodular shape. Rim enhancement is frequently seen in PFTCs with a tubal component, which may suggest a tubal origin.

Keywords Fallopian tube neoplasms · Magnetic resonance imaging · Diffusion MRI

Introduction

Primary fallopian tube cancer (PFTC) was long thought to be a rare tumor that accounts for 0.7–1.5% of all gynecologic malignancies [1]. PFTC was pathologically diagnosed based on the modified criteria of Hu et al. [2] and Sedlis [3]: (1) the main tumor lies in the tube and arises from the endosalpinx; (2) histologically, the pattern resembles the tube mucosa and is often papillary; (3) if the wall of the fallopian tube is involved, the transition from benign to malignant epithelium must be demonstrated; and (4) the ovaries and uterus are normal or contain less tumor than the tubes. The most common histological type of tubal carcinoma is high-grade serous carcinoma (HGSC) [1]. Recently, however, several studies have suggested that a significant subset of HGSC in the ovaries may derive from serous tubal intraepithelial carcinoma (STIC) [2–6]; so-called classical PFTC, which meets the criteria mentioned above, is rare. Classical PFTCs are often symptomatic [1, 7, 8], with a mean age ranging from 56 to 63 years [1]. In one study of 151 patients with PFTC, 86% patients were postmenopausal [9]. The common symptoms are vaginal bleeding and discharge (50–60% of patients), followed by abdominal pain (30–49% of patients) and an abdominal mass (12–61% of patients) [7]. However, the clinical presentation of patients with classical PFTC may be similar to those of patients with ovarian cancer or endometrial cancer, making preoperative diagnosis of PFTC difficult [7, 8]. Additionally, a positive Pap smear is observed in 10–36% of PFTC cases [7], which can lead to an incorrect diagnosis, such as cervical or endometrial cancer. The principles of PFTC management generally follow those of epithelial ovarian cancer [1, 7, 8, 10]. Clinically, preoperative differentiation between ovarian cancer and PFTC is not mandatory [7, 8], although detecting an adnexal cancer and differentiating between PFTC and uterine cancer are important.

Magnetic resonance imaging (MRI) findings for PFTC are reportedly a relatively small solid mass with a sausage-like shape and restricted diffusion [11–13]. However, reports of

✉ Satomi Kitai
kitai@jikei.ac.jp

[1] The Jikei University School of Medicine, 3-25-8 Nishi-shimbashi, Minato-ku, Tokyo 158-0001, Japan

MRI findings for PFTCs are still scarce. In our experience, rim enhancement of the tumor is often seen on enhanced MRI. Therefore, the purpose of this study was to clarify the imaging characteristics of PFTCs.

Materials and methods

Patients

This retrospective study was approved by our institutional review board, and informed consent was waived. The pathological database with patients registered between May 2007 and February 2016 was searched, and 29 patients who were pathologically diagnosed with PFTC were found. Inclusion and exclusion criteria are shown in Fig. 1. Of the 29 patients found, 8 patients with microscopic PFTC and another 6 patients with both ovarian and tubal carcinomas, whose primary sites could not be determined, were excluded. Fifteen patients had so-called classical PFTC. MRI was available in 11 of 15 cases in our picture archiving and communication system (PACS). MRI quality was adequate in all 11 patients. The primary tumor was resected within 40 days of MRI assessment in 10 patients, and after 124 days of initial MRI assessment in one patient who had interval debulking surgery (IDS).

Clinical and pathological findings are summarized in Table 1. The patients ranged in age from 50 to 69 years (median 62 years). None of them had a history or family history of breast or ovarian cancer. Staging was performed according to the International Federation of Gynecology and Obstetrics (FIGO) staging system [10] and gave the following results: two patients were stage I; seven patients were stage III; and the remaining two patients were stage IV. Endometrial and/or cervical cytology was positive in three patients and endometrial curettage was performed in two patients; malignancy was not detected with either method. PFTC was suspected before MRI examination

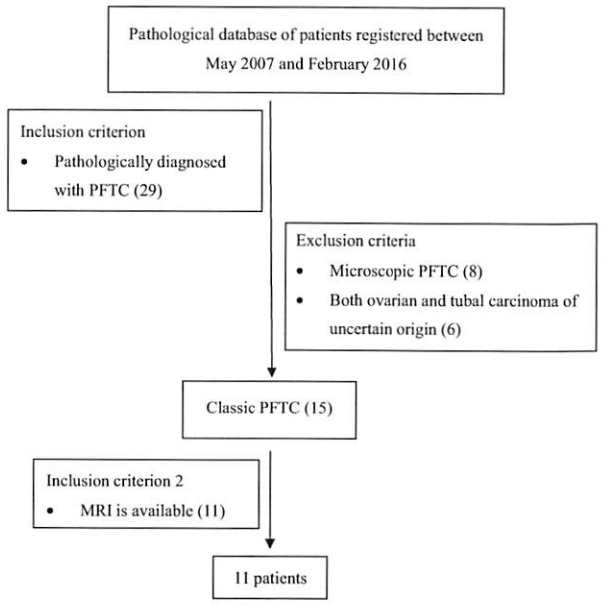

Fig. 1 Inclusion criteria

Table 1 Clinical and pathological findings

Clinical or pathological finding	Number
Mean age [SD] (years)	62 [6.0]
Menstruation status	
Postmenopausal	9
Premenopausal	1
Post TAH	1
Symptoms	
Vaginal bleeding or discharge	6
Abdominal pain, discomfort, or swelling	5
Anorexia	1
Asymptomatic	1
Serum Ca-125 elevation	10
Cytology positivity	
Endometrium	3
Cervix	1
Mean greatest tumor dimension [SD] (cm)	3.3 [1.8]
Histological subtype	
HGSC	10
Clear cell carcinoma	1
Macroscopic PFTC location	
Ampulla	1
Ampulla or distal portion to fimbria	7
Fimbria	3
Presence of STIC	9
Depth of tumor invasion	
Muscularis propria	2
Subserosa	3
Serosa and surrounding tissue	4
Confined to the fimbria	2
FIGO stage	
I	2
II	0
III	7
IV	2
Postsurgical status	
Complete	6
Optimal	1
Suboptimal	4

FIGO stage International Federation of Gynecology and Obstetrics staging, *HGSC* high-grade serous carcinoma, *SD* standard deviation, *SI* signal intensity, *STIC* serous tubal intraepithelial carcinoma

in one patient, while endometrial cancer was suspected in three patients. After MR examination, PFTC was suspected in seven patients. The histological subtype was HGSC in ten patients and clear cell carcinoma (CCC) in one patient. Macroscopically, the tumor had a tubal component in eight cases (at the ampulla in one case, and the ampulla/distal portion to the fimbria in seven cases) and at the fimbria in three cases. Histologically, the depth of tumor invasion was to the muscularis propria in two cases, the subserosa in three cases, the serosa and surrounding tissue in four cases, and was confined to the fimbria in two cases. Ipsilateral ovarian involvement was seen in five cases, and was microscopic in all cases.

MRI examination

MRI examinations of eight patients were performed in our institution using a 1.5-T scanner (MAGNETOM Avanto or MAGNETOM Symphony; Siemens, Erlangen, Germany). MRI examinations of an additional three patients were performed at an outside clinic; the scanner used was not known. T2-weighted images (T2WI, turbo spin echo) in the axial and sagittal planes were available for all patients. Diffusion-weighted images (DWI, echo planar imaging) were available in the axial plane for all patients, with apparent diffusion coefficient (ADC) maps obtained for ten patients. The corresponding *b* values of the diffusion sensitizing gradient were 50 and 800 mm^2/s in our institute, but it is not known what they were in the outside clinic. Axial images were set to a uniform section thickness of 4.0–7.0 mm, with an intersection gap of 0–6.0 mm and a field of view (FOV) of 30–38 cm. Sagittal images were set to a uniform section thickness of 4.0–6.0 mm, with an intersection gap of 0–3.5 mm and a FOV of 26–30 cm. Totally enhanced MRI was available for nine patients, including eight dynamic contrast-enhanced (DCE) studies. DCE MR images were obtained in either the sagittal or the axial plane at 0, 25, 70, and 150 s, or at every 20 s until 120 s (slice thickness 2.0–3.0 mm, without a gap). An intravenous (IV) bolus injection (2 mL/s) of 0.2 mL/kg body weight of gadopentetate dimeglumine (Magnevist®, Bayer HealthCare Pharmaceuticals, Berlin, Germany) or gadodiamide hydrate (Omniscan®, Daiichi-Sankyo Pharmaceuticals, Tokyo, Japan) was given in our institute. After the dynamic study, fat-suppressed T1-weighted images (T1WI, volumetric interpolated breath-hold examination, slice thickness 2.5–3.0 mm; without a gap; FOV 35 cm) were obtained at 180 s in either the axial or the sagittal plane; these were not taken in the dynamic study. Contrast-enhanced fat-suppressed T1WI (spin echo, slice thickness 6.0 mm; without a gap) in the axial plane was available for one patient.

Imaging analysis

MRI findings were retrospectively reviewed by two radiologists (S.K. and K.O., both with more than 10 years of experience in abdominal imaging) with a knowledge of the pathological findings. The reviewers evaluated all images together, and agreement was reached in conference after careful individual evaluation.

MR imaging of the tumor was studied, including size, shape, appearance, signal intensity, and enhancement pattern, hydrosalpinx, and location, as well as the morphologic appearance of the ipsilateral ovary and intrauterine fluid collection. As for the size, the longest and shortest diameters were measured on the axial or sagittal T2WI, in which the tumor was visualized in the greatest dimension. The shape of the tumor was classified as sausage-like, irregular, or nodular. Sausage-like was defined as a curved elongated shape with a round cut-surface, in which the longest diameter was more than twice the shortest diameter (Fig. 2a). Other tumors were divided based on the contour into nodular (Fig. 2b) or irregular (Fig. 2c). They were further divided by appearance into solid or solid and cystic. Solid was defined as a solid tumor without cysts (Fig. 2d); solid and cystic was defined as a tumor with combined solid and cystic components (Fig. 2e-1) or a solid tumor containing cysts (Fig. 2e-2). Signal intensities of the solid portion on T2WI and DWI/ADC maps were evaluated by comparison with those of the outer myometrium, except in one post-hysterectomy case, where the signals were compared to those of the skeletal muscle instead. The mean ADC values ($\times 10^{-3}$ mm^2/s) were evaluated in eight cases in which the MRI was taken in our hospital with a known *b* value. The mean ADC value ($\times 10^{-3}$ mm^2/s) of the solid portion of the tumor was measured in a circular region of interest in one representative region that was as large as possible within the tumor from the ADC maps using a workstation (Syngo Imaging, Siemens). The presence of rim enhancement, which was linear enhancement around the tumor, was evaluated. The degree of rim enhancement was compared with the outer myometrium. On DCE MRI, the circular ROI was placed in the solid portion of the tumor (avoiding the rim enhancement) in one representative region that was as large as possible using a workstation (Syngo Imaging). The signal intensity of the solid portion was measured before and 60/70 s after IV injection of gadolinium contrast material. The percentage increase in signal intensity at 60/70 s was calculated. Early enhancement was defined as an increase in signal intensity of 100% or more within the first 70 s. Marked enhancement was defined as an enhancement that was similar to or more than the myometrium at 20–70 s, except for rim enhancement. The presence of hydrosalpinx and intrauterine fluid collection was evaluated on T2WI and/or contrast-enhanced T1WI. Intrauterine fluid collection volumes were

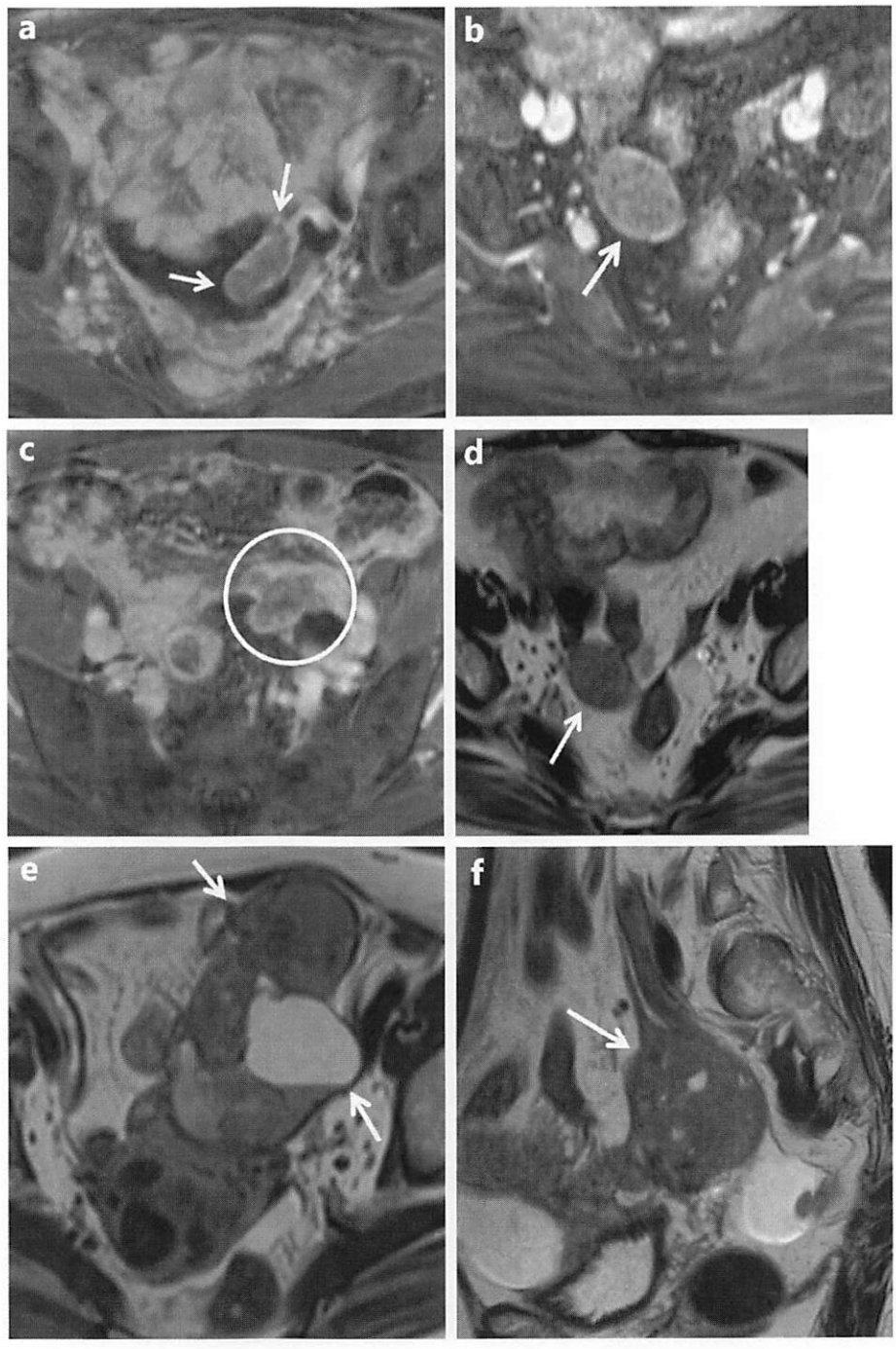

Fig. 2a–f Samples of the shapes (**a–c**) and appearances (**d–f**) of PFTCs. **a** Sausage-like. **b** Nodular. **c** Irregular. **d** Solid. **e**, **f** Solid and cystic. A tumor with solid and cystic components is shown in **e** and a solid tumor containing cysts in **f**

divided into small or large volumes based on the thickness of the enlarged uterine cavity on a sagittal image as follows: >1 cm, large; ≤1 cm, small. The location of the tumor in relation to the uterus was evaluated and described as follows: in contact with the uterus with/without the interstitial portion of the fallopian tube, or separate from the uterus. Ipsilateral ovary identification, size, and appearance (nodular or irregular) were also performed/evaluated on MRI.

Finally, MRI findings and pathological findings including histological subtype, macroscopic tumor location, depth of the tumor invasion, and ovarian involvement were compared.

Results

The MRI findings are summarized in Table 2. The greatest tumor dimension ranged from 1.7 to 9.2 cm, with a mean diameter (SD) of 4.2 (1.8) cm. The shortest tumor dimension ranged from 1.2 to 5 cm, with a mean diameter (SD) of 2.6 (1.1) cm. Five tumors were sausage-shaped, and these all had a tubal component macroscopically (Fig. 3). The other three tumors with a tubal component had a nodular or irregular shape. Three tumors located at the fimbria presented a nodular shape (Fig. 4). The tumors were solid in nine patients (82%). In one patient with a solid and cystic tumor, the cystic portion was found to be a paratubal cyst.

The solid portions of the PFTCs showed high signal intensities on DWI in all patients. Low signal intensities were observed on the ADC maps for nine HGSCs (Fig. 3), and iso signal intensities were seen for the clear cell carcinoma (CCC). The ADC value for the CCC (1.52×10^{-3} mm^2/s) was higher than the average ADC value for HGSC (0.77×10^{-3} mm^2/s), even when calculated without areas of necrosis or degeneration.

Early enhancement was noted in six of eight patients. Marked enhancement was seen in two patients. Rim enhancement (i.e., as enhanced or more strongly enhanced than myometrium at every phase of the DCE study) was observed in six of nine patients. Pathologically, all tumors with rim enhancement had an intratubal component and a dilated tube, in which focal invasion of the muscularis propria or the serosa of the tubal wall or small tumor foci on the serosal surface were seen. Otherwise, the tubal wall was preserved (Fig. 3). Three tumors without rim enhancement were located at the fimbria (Fig. 4).

On MRI, the tumors were in contact with the uterus in seven patients, but they were not observed at the interstitial portion of the fallopian tubes or attached to the conus of the uterus. Pathologically, none of the tumors were located at the interstitial portion or proximal portion of the fallopian tubes. The ipsilateral ovary was identified in four patients. This was nodular in all patients and its greatest diameter ranged from 1.0 to 1.8 (average 1.2) cm. It was pathologically intact in three patients and contained microscopic metastases in one patient. In seven patients, the ipsilateral ovary could not be identified. Pathologically, metastases were found in only one patient.

Hydrosalpinx was seen in only two patients. Intrauterine fluid collection was observed in five patients. The volume of intrauterine fluid collection was small in four patients and large in one patient in whom metastatic cervical tumor was noted (Fig. 3d).

Table 2 Imaging features

Imaging feature (evaluation cases)	Number
Mean greatest tumor dimension [SD] (cm)	4.2 [1.8]
Shape (11)	
Sausage-like	5
Nodular	4
Irregular	2
Appearance (11)	
Solid	9
Solid and cystic	2
SI of solid component (11)	
Iso/mildly hyperintense on T2WI (11)	11
Hyperintense on DWI (11)	11
Hypointense on ADC map (10)	10
Average mean ADC value (8)	0.86
Average mean ADC value of HGSC (7)	0.77
Mean ADC value of clear cell carcinoma (1)	1.52
Enhancement (9)	
Early enhancement (8)	6
Marked enhancement (8)	2
Rim enhancement (9)	6
Hydrosalpinx (11)	2
Intrauterine fluid collection (10)	5
Location: position in relation to the uterus (10)	
Contact with uterus (interstitial portion)	7 (0)
Separate from the uterus	3
Identification of the ipsilateral ovary (11)	4

HGSC high-grade serous carcinoma, *SD* standard deviation, *SI* signal intensity

Discussion

The present study showed that a sausage-like shape is exhibited by PFTCs with a tubal component, and a nodular shape is displayed by PFTCs located at the fimbria. Rim enhancement is frequently seen in PFTCs with a tubal component and may suggest a tubal origin.

In the literature, MRI findings for PFTC are characterized by a relatively small adnexal tumor that measures 3–12 cm in greatest diameter and is solid or solid and cystic if associated with hydrosalpinx [11, 12, 14]. It has been reported that a sausage-like/fusiform/serpentine shape is seen in 70% of cases, and a nodular/irregular shape is seen in 30% of cases, while a sausage-shaped tumor is not seen in patients with epithelial ovarian cancer [13]. Based on our results, a sausage shape for the tumor appears to indicate the presence of a tubal component. Only five cases (45%) in our series had a sausage-shaped tumor, but this may be due to differences in tumor shape interpretation, as this is yet to be explored in detail. PFTC may also form a nodular or irregularly shaped tumor, especially when the tumor is confined to the fimbria.

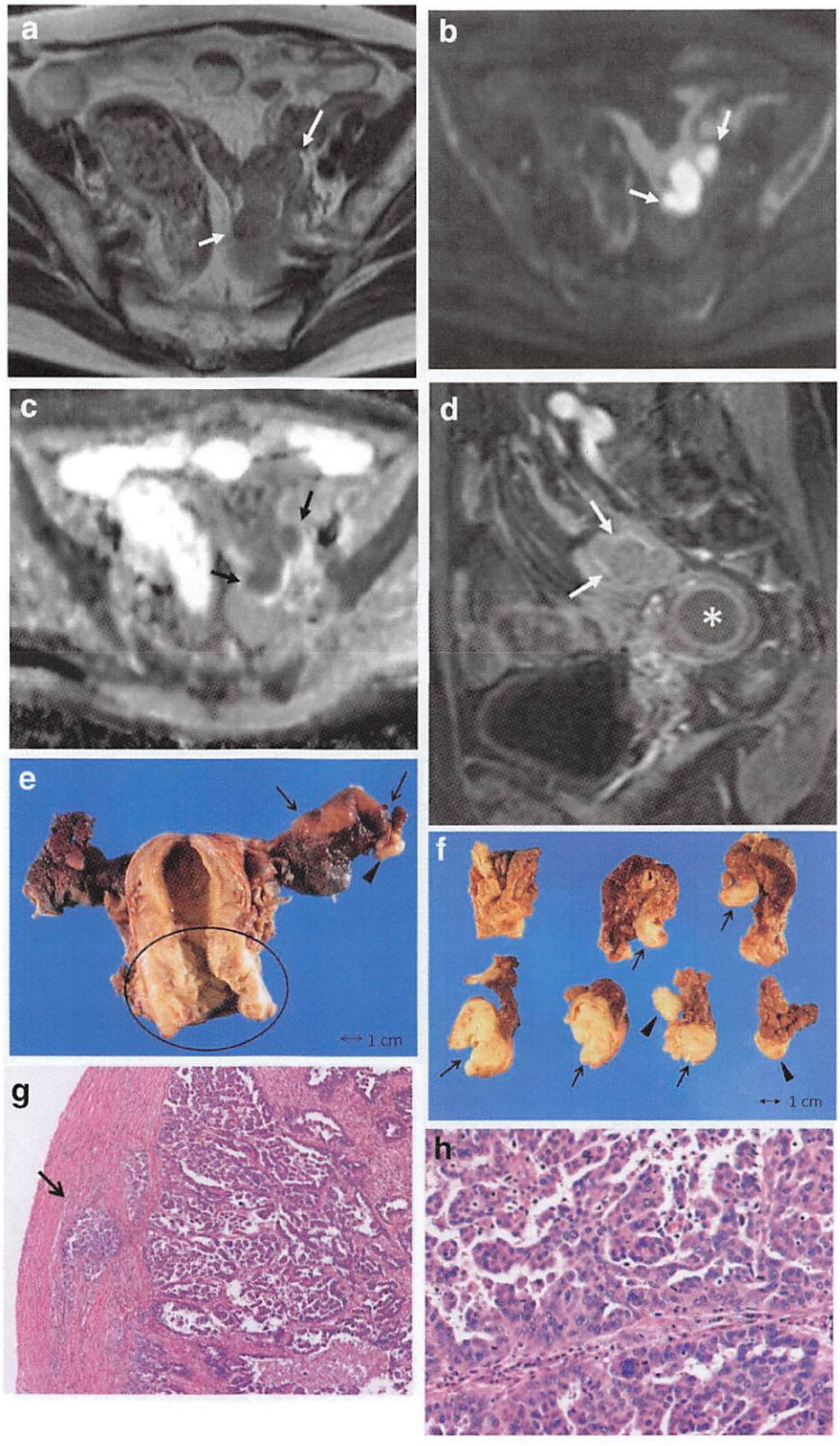

Fig. 3a–h Left primary fallopian tube cancer (case 1, HGSC, FIGO stage III A1). **a–c** A sausage-shaped tumor in the left adnexal area displays moderately high SI on a T2-weighted axial image (*arrows* in **a**), high SI on DWI (*arrows* in **b**), and low SI on the ADC map (*arrows* in **c**). **d** Gadolinium-enhanced fat-suppressed T1-weighted VIBE image at 70 s shows rim enhancement of the tumor (*arrows*). An intrauterine fluid collection is noted (*asterisk*). **e** Macroscopic findings of the resected uterus and bilateral adnexae. The fallopian tube is enlarged from the ampulla to the fimbria (*arrows*), and whitish tumor is noted in the fimbria (*arrowheads*). The uterine cervix is thickened by the tumor (*circle*); it was found to be metastatic carcinoma from the left fallopian tube. **f** Cross-sections of the left fallopian tube. Whitish solid tumor occupies the lumen of the fallopian tube (*arrows*) and the fimbria (*arrowheads*). **g, h** Hematoxylin–eosin (HE) staining of the tubal tumor. The tumor grows in the tubal lumen and invades the muscularis propria of the tube (*arrow* in **g**). A higher-magnification image (**h**) presents pleomorphic tumor cells showing invasive growth with papillary formation

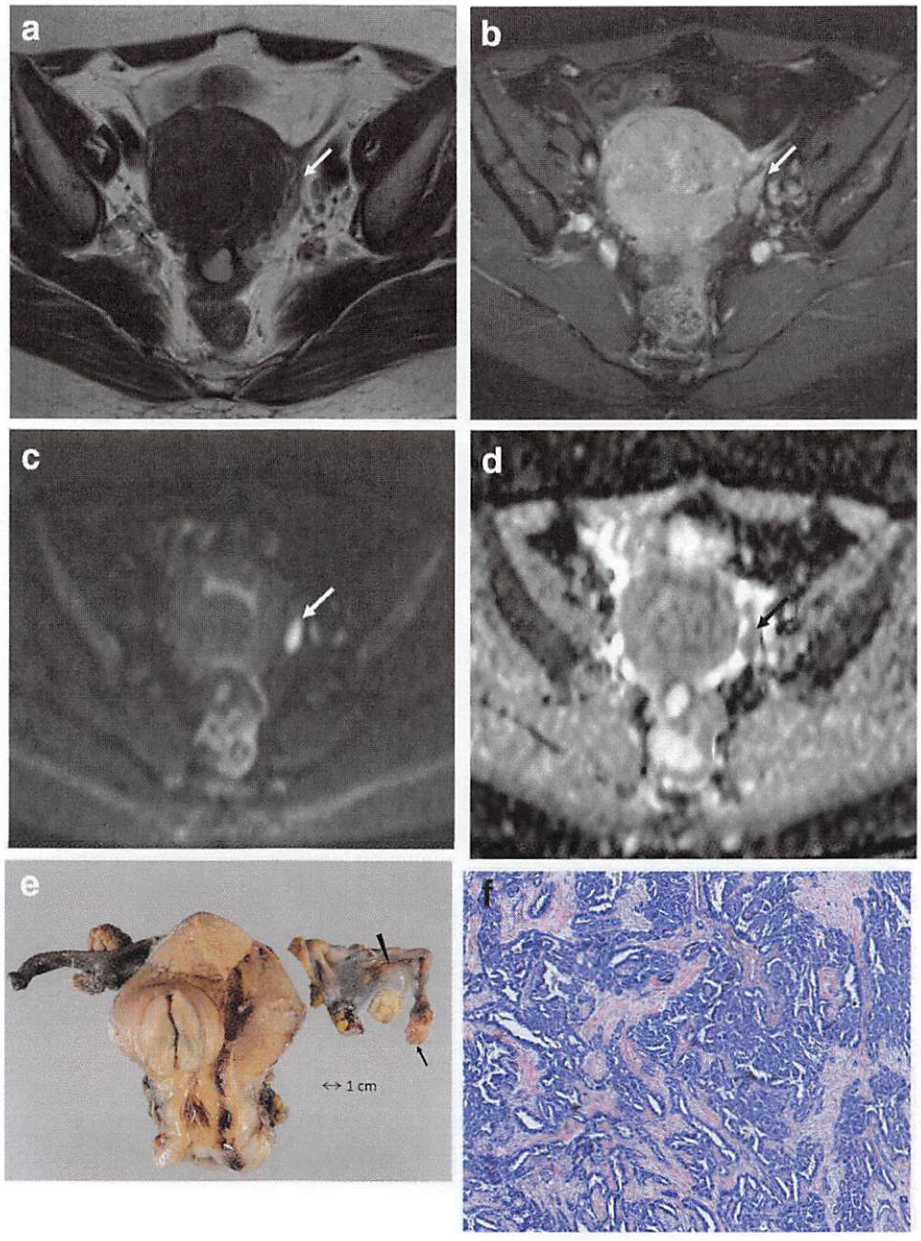

Fig. 4a–f Left primary fallopian tube cancer (case 10, HGSC, FIGO stage III C). **a** T2-weighted axial image shows an adnexal tumor with a nodular shape, which displays moderately high intensity (*arrow* in **a**). **b–d** The tumor shows marked early enhancement at 60 s (*arrow* in **b**), high SI on DWI (*arrow* in **c**), and low SI on the ADC map (*arrows* in **d**). **e** Resected uterus and bilateral adnexae. Whitish solid tumor is noted in the fimbria (*arrow*). A paratubal cyst is also seen (*arrowhead*). **f** HE stain of the tubal tumor. Columnar epithelial cells with a high N/C ratio and high atypia that invade in a papillary pattern with tubal formation indicate high-grade serous carcinoma

PFTC was reported to occur most often in the distal two-thirds and to be confined to the fimbria in a few cases [15]. On MRI, these tumors were adjacent to the uterus but were not present at the interstitial portion of the fallopian tube, suggesting that the tumors initially occur at the distal portion rather than at the proximal portion of the fallopian tube. Since the distal fallopian tube is close to the ovary, PFTC is often difficult to differentiate from ovarian tumor. However, the presence of a sausage-shaped mass in the adnexal area on MRI may suggest PFTC. In a few patients, the ipsilateral ovary may be identifiable, just as in the present series.

The solid lesion of a PFTC shows a homogeneous, relatively hyperintense signal similar to that of uterine myometrium on T2WI [11, 12]. On DWI, the solid portion of a PFTC shows high intensity, with low intensity observed on ADC maps [12]. In the recent report and in the present series, even the smallest tumor, which was 14 and 17 mm in greatest dimension, respectively, showed high signal intensity on DWI [12]. DWI is also capable of detecting endometrial or cervical carcinomas [16, 17], and it may differentiate PFTC from uterine carcinomas in patients with vaginal bleeding and/or positive cervical or endometrial cytology. One patient with clear cell carcinoma showed a

higher intensity on ADC maps compared to serous carcinomas, probably due to histological differences and decreased cellular density.

With the use of contrast media in MRI, it has been reported that the solid portion of PFTC shows mild to obvious homogeneous enhancement [11, 12]. The enhancement pattern of PFTC is similar to that seen in ovarian carcinoma [18], but obvious enhancement is more likely to be seen in EOC [13]. Rim enhancement of the tumor was reported to be observed on enhanced CT [11], and it was observed in six of nine enhanced cases in the present study, reflecting the tubal wall. This finding may aid in the diagnosis of PFTC.

Intrauterine fluid collection has been reported to be an imaging feature associated with PFTC on CT and MRI [11, 13]. It was seen in five patients in the present study, and only a small amount of intrauterine fluid accumulation was observed in four of those cases. Thus, careful examination on MRI—especially T2WI and delayed contrast-enhanced studies—is required to evaluate intrauterine fluid collections.

Finally, the MRI findings that were highlighted in this study may indicate the possibility of PFTC, and preoperative MRI may represent more appropriate management, especially in patients with PFTC who are clinically suspected to have uterine cancer.

There are several limitations of this study. First, it was a retrospective study with patient bias and variable MRI protocols. Second, its sample size was small, and further studies with more cases will be needed to determine the comprehensive imaging features of PFTC. Third, only cases that met the criteria of Hu et al. [2] and Sedlis [3] were evaluated, and small PFTCs with larger ovarian/peritoneal tumors may also be identified as imaging features of PFTCs in the future.

Conclusion

A sausage-shaped tumor is typical of PFTCs with a tubal component, and a tumor with a nodular shape is seen in PFTCs located at the fimbria. Rim enhancement is frequently seen in PFTCs with a tubal component, which may suggest a tubal origin.

Acknowledgements The authors would like to thank the radiology technicians at our institute, especially Mr. Keiji Noguchi, for their work to obtain precise MR images. The authors would also like to thank the staff of FORTE Science Communications (Tokyo, Japan) (https://www.forte-science.co.jp/) for their English language editing of the manuscript.

Compliance with ethical standards

Conflict of interest The authors declare that they have no conflict of interest.

Ethical statement This retrospective study was approved by our Institutional Review Board, and informed consent was waived.

Funding This paper has not been funded.

References

1. Vang R, Wheeler JA. Disease of the fallopian tube and paratubal region. In: Kurman RJ, Ellenson LH, Ronnett BM, editors. Blaustein's pathology of the female genital tract. 6th ed. New York: Springer; 2011. p. 554–69.
2. Hu CY, Taymor ML, Hertig AT. Primary carcinoma of the fallopian tube. Am J Obstet Gynecol. 1950;59:58–67.
3. Sedlis A. Carcinoma of the fallopian tube. Surg Clin N Am. 1978;58:121–9.
4. Colgan TJ, Murphy J, Cole DE, Narod S, Rosen B. Occult carcinoma in prophylactic oophorectomy specimens: prevalence and association with BRCA germline mutation status. Am J Surg Pathol. 2001;25:1283–9.
5. Medeiros F, Muto MG, Lee Y, Elvin JA, Callahan MJ, Feltmate C, et al. The tubal fimbria is a preferred site for early adenocarcinoma in women with familial ovarian cancer syndrome. Am J Surg Pathol. 2006;30:230–6.
6. Kindelberger DW, Lee Y, Miron A, Hirsch MS, Feltmate C, Medeiros F, et al. Intraepithelial carcinoma of the fimbria and pelvic serous carcinoma: evidence for a causal relationship. Am J Surg Pathol. 2007;31:161–9.
7. Ajithkumar TV, Minimole AL, John MM, Ashokkumar OS. Primary fallopian tube carcinoma. Obstet Gynecol Surv. 2005;60:247–52.
8. Pectasides D, Pectasides E, Economopoulos T. Fallopian tube carcinoma: a review. Oncologist. 2006;11:902–12.
9. Baekelandt M, Jorunn Nesbakken A, Kristensen GB, Tropé CG, Abeler VM. Carcinoma of the fallopian tube. Cancer. 2000;89(10):2076–84.
10. Prat J, FIGO Committee on Gynecologic Oncology. Staging classification for cancer of the ovary, fallopian tube, and peritoneum. Int J Gynecol Obstet. 2014;124:1–5.
11. Kawakami S, Togashi K, Kimura I, Nakano Y, Koshiyama M, Takakura K, et al. Primary malignant tumor of the fallopian tube: appearance at CT and MR imaging. Radiology. 1993;186:503–8.
12. Cai SQ, Ma FH, Qiang JW, Zhao SH, Zhang GF, Rao YM. Primary fallopian tube carcinoma: correlation between magnetic resonance and diffuse weighted imaging characteristics and histopathologic findings. J Comput Assist Tomogr. 2015;39:270–5.
13. Ma FH, Cai SQ, Qiang JW, Zhao SH, Zhang GF, Rao YM. MRI for differentiating primary fallopian tube carcinoma from epithelial ovarian cancer. J Magn Reson Imaging. 2015;42:42–7.
14. Mikami M, Tei C, Kurahashi T, Takehara K, Takehara K, Komiyama S, et al. Preoperative diagnosis of fallopian tube cancer by imaging. Abdom Imaging. 2003;28:743–7.
15. Alvarado-Cabrero I, Stolnicu S, Kiyokawa T, Yamada K, Nikaido T, Santiago-Payán H. Carcinoma of the fallopian tube: results of a multi-institutional retrospective analysis of 127 patients with evaluation of staging and prognostic factors. Ann Diagn Pathol. 2013;17:159–64.
16. Tamai K, Koyama T, Saga T, Umeoka S, Mikami Y, Fujii S, et al. Diffusion-weighted MR imaging of uterine endometrial cancer. J Magn Reson Imaging. 2007;26:682–7.
17. Liu Y, Bai R, Sun H, Liu H, Wang D. Apparent diffusion coefficient in cervical cancer of the uterus: comparison with the normal uterine cervix. J Comput Assist Tomogr. 2009;3:858–62.
18. Thomassin-Naggara I, Balvay D, Aubert E, Daraï E, Rouzier R, Cuenod CA, et al. Quantitative dynamic contrast-enhanced MR imaging analysis of complex adnexal masses: a preliminary study. Eur Radiol. 2012;22:738–45.